Middle-East Journal of Scientific Research 20 (11): 1402-1412, 2014
ISSN 1990-9233

DOI: 10.5829/idosi.mejsr.2014.20.11.1035

Electrical Properties of Doped Azopolyester

[1]K. Gopalakrishnan, [2]J. Sundeep Aanand and [3]R. Udayakumar

[1]Electronics Communication Engineering, Bharath University, Chennai-73, India
[2]Computer Science Engineering, Bharath University, Chennai-73, India
[3]School of Computing Sciences, Bharath University, Chennai-73, India

Abstract: The conduction measurements in polymers are very much dependent on defects in polymer chains and the disorder order created by dopant ions. The presence of localized electronic states of energies less than the band gap arising from charges in local bond including the formation of solitons, polarons and bipolaron have lead to the possibility of new types of charge conduction present in the polymer systems. The former tends to occur at high frequencies, where the carriers excited beyond mobility edges into non-localized states dominate the transport and band edges. In either case, the position of the Fermi-level [E_f] is of very important. Electrical properties of doped Azopolyester are studied with the help of Schottky Richardson emission, Poole-Frenkel emission, observed that the AC conductivity of the polymeric blend films obeys the correlated barrier hopping (CBH) model and the solid lines are the straight line fits obtained by the least squares fitting procedure results. When the frequency increases conductivity also increases.

Key words: Dopant ions · Bipoloran · Fermi-level · Solitons · Band gap

INTRODUCTION

Zuo *et al*. [1] have made an extensive study on temperature dependence of the DC and AC conductivity of the polymers.

Aromatic acids doped with PANI at different dopant levels were studied by Rahunathan *et al*. [2]. Kahol *et al*. [3] investigated that the electron localization behavior of polyaniline as a function of dopant type. Systematic studies on doped Azopolyester blends show the variation of DC conductivity with temperature. By changing parameters like electric field, pressure, magnetic field and in some cases, mechanical stress, the position of the fermi level and the structure of the thin film can be changed. Consequently, the transport processes may switch over from one state to another by depending on the external parameters. For example, hopping or tunneling of charge carriers take place in low electric field and the conduction processes such as thermionic or Schottky Richardson emission, Poole-Frenkel emission, etc are mainly controlled by the high electric filed. The transport of charge carriers (electrons, holes) in these systems could be characterized either by band controlled conduction or by a succession of hopping from one site to another.

DC Conduction Process in Doped Azopolyester

Hopping Conduction Technique: Conducting polymers are polycrystalline (or) amorphous in nature and they have a substantial amount of disorder. The disorder arises during the synthesis and processing due to presence of partial crystalline, impurities and lack of long range order etc. When the charge carriers are localized due to random electric fields, instead of band conduction charge transport takes place between hopping of localized sites are shown in the Figure 1.

Since the localized states have quantized energies extending over a certain range, activation energy is required for each hopping. Hopping occurs either near the Fermi level or near the maximum density of states. Hopping near the Fermi level dominates at low temperatures. Hopping near the maximum density of states dominates at high temperatures. Generally an

Corresponding Auhtor: R. Udayakumar, School of computing Sciences, Bharath University, Chennai-73, India.

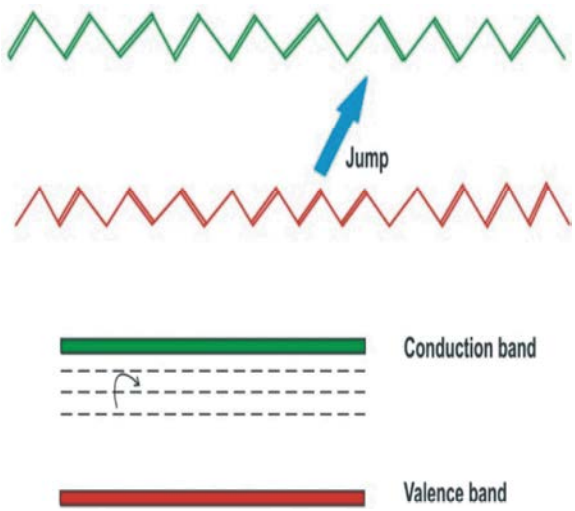

Fig. 1: Principle of variable range hopping mechanism illustrates by the charge transfer between two adjacent chains

electron of a hole prefers hop to a more remote site than to the neighbor one, in order to reduce the energy required for the hopping is called variable range hopping [VRH] [4].

The simplest approach of Mott considers two localized sites; one filled laying slightly below the Fermi level (E_f) and the other empty, which lines above E_f. Mott has defined the hopping transition rate as

$$\gamma = V_o \exp\left(-2\alpha R - \Delta l k_B T\right) \tag{1}$$

where *exp (-Δ/K_BT)* is the probability for the existence of a phonon of energy *(Δ) exp (-2αR)* is the probability for the charge carrier to transfer by tunneling, V_o is the attempt frequency and depends on the strength of electron phonon coupling and the phonon density of states but weakly depends on hopping distance *(R)* and Δ. α^{-1} is the spatial extension of the wave function associated with the localized states k_B is the Boltzmann's constant and T is the absolute temperature. Mott has also defined the hopping conductivity (σ) as

$$\sigma = e^2 \frac{R^2}{6} V_o \exp\left(-2\alpha R - \Delta l k_B T\right) \tag{2}$$

At low temperatures, where both the number and energy of phonons are small, hopping to the nearest neighbor is unfavorable, because of the larger energy separations encountered on average. Instead, it is more favorable for the charge carrier's tunnel to more distant sites, which will have smaller energy separation. This type of long-range hop is known as variable range hopping [VRH] process [5].

To derive the conductivity equation for variable range hopping process, Mott has considered that the factor *(2αR + Δk_B/T)* should be optimized, subject to the condition that there is at least one state at a given spatial and energy separation that is

$$\frac{4\pi}{3} N\left(E_F\right) \Delta R^3 = 1 \tag{3}$$

Introducing the equation (3) into the factor [2αR+Δk_B/T], then maximization of the exponent yielded a formula for an optimum hopping distance (R) as

$$R = \left[\frac{9}{8\pi\alpha k_B N(E_F) T}\right]^{1/4} \tag{4}$$

the optimized energy separation can be obtained from equation (3) as

$$\Delta = \frac{3}{4\pi R^3 N(E_F)} \tag{5}$$

when both R and Δ values inserted into an equation 2, then that equation yields a final expression for a hopping conductivity at low temperature as

$$\sigma_{dc} = \sigma_o \exp\left[-\left(\frac{T_o}{T}\right)^n\right] \tag{6}$$

where n=1/4 for three dimensional (3D) VRH model. The pre-exponential factor σ_o and the characteristic temperature T_o are related to the density of localized states $N(E_F)$ also the wave function decay constant α associated with these states by the following relations.

$$\sigma_o = \left[\frac{A^2 N\left(E_F\right)}{\alpha}\right]^{1/2} \tag{7}$$

where $A = \left[\frac{3e^2 V_{ph}}{\sqrt{8\pi k_B}}\right]$ a complex parameter and is the Mott temperature is 3D and it is given by

$$T_o = \frac{16\alpha^3}{k_B N(E_F)} \tag{8}$$

where k_B is the Boltzmann constant (1.38054 x 10^{-23} J/K) and V_{Ph} is the phonon frequency [$\approx 10^{13}$ H_Z]. The expression for range of hopping in three dimensions is given by

$$R_{hop}(T) = \frac{3}{8}\left[\frac{T_0}{T}\right]^{1/4} \alpha^{-1} \tag{9}$$

and the activation energy for hopping is given by

$$W_{hop} = k_B (T_o T^3)^{1/4} \tag{10}$$

According to eqn. (6), if a plot between $ln\ \sigma(T)\ T^{1/2}$ versus $T^{-1/4}$ obeys a linear relationship, then the conductivity in that temperature range is said to be 3D variable range hopping type.

According to one dimensional (ID) VRH model, the temperature dependent conductivity is similar to equation (6), where the temperature index n = ½, T_o generally depends on the electronic states and the energy distribution of localized states, which is related to the inverse localization length (α), most probable hopping distance (R_{hop}) and hopping energy [W_{hop}] by the following relations (11), (12) and (13)

$$T_o = \frac{8\alpha}{k_B N(E_F) Z} \tag{11}$$

$$R_{hop} = \frac{1}{4}\left[\frac{T_0}{T}\right]^{1/2} \alpha^{-1} \tag{12}$$

$$W_{hop} = \frac{Z k_B T_o}{16} \tag{13}$$

where Z is the number of nearest neighboring chains [≈4 for PANI] k_B is the Boltzmann constant and $N(E_F)$ is the density of states per eV (2-ring units suggested for doped Azopolyester).

DC Measurement Techniques: For DC conduction measurement the three different doped Azopolyester thin films of same thickness of 5.2 µm were formed by solution casting technique with silver paste (highly conducting paste - supplied by Eltecks Corporation, Bangalore) as top and bottom electrodes to form a parallel plate structure [6].

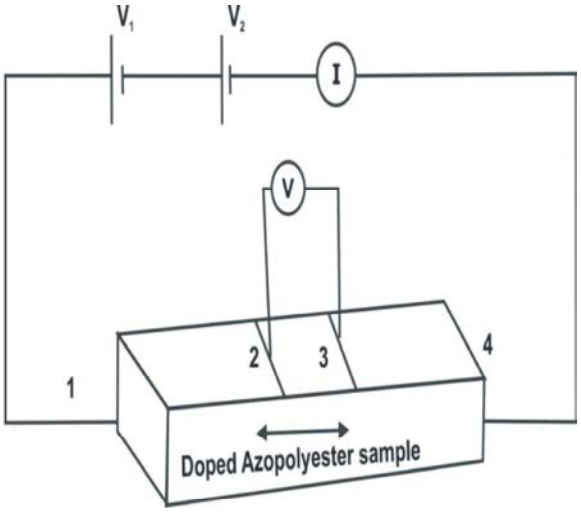

Fig. 2: Connection diagram of four probe resistivity measurement

The silver paste as electrode was deposited at room temperature by vacuum ($2.8x10^{-3}$pa) evaporation. A PT100 thermocouple connected with the temperature controller is maintaining the required temperature with a precision of 0.5K. The current-voltage source coupled with a high input impedance electrometer [Lab Equip, India].A four-probe, Keithley measuring unit were used to apply voltage of -20 to + 20 V in steps of 0.01 V.

Now to applying of each voltage increment, current was automatically measured with a delay time of 2 second. I-V data at each selected temperature was transferred through a GPIB interface to PC and stored for further analysis.

The current through the capacitor as a function of applied voltage was measured in a rotary vacuum (≈1.33pa) at different temperature ranging from 303-343K.

Four-Point Probe Instrument: The four-point probe consists of two current carrying probes (1&4) and two voltage measuring probes (2&3) since contact of sample and spreading resistance is associated with the voltage probes [7].

The resistivity of the pellet is calculated at different temperatures using the given formula.

$$\rho = \frac{1}{G_7\left(\frac{W}{S}\right)} \times \frac{V}{I} \times 2\pi S \tag{14}$$

where S is the distance between the probes (S=0.2cm) W is the thickness of the sample and

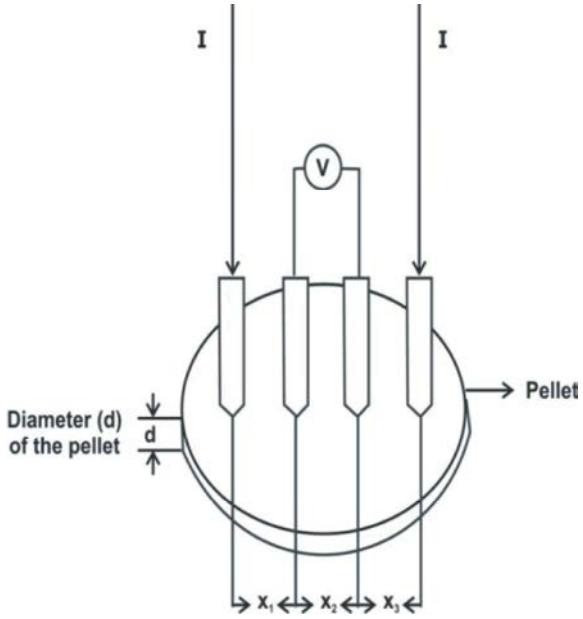

Fig. 3: Schematic representation of a resistivity measurement with a four point probe Instrument

$$G_7 = \left(\frac{W}{S}\right) = \frac{2S}{W}\log e^2 \tag{15}$$

Conductivity can be computed using the relationship σ = 1/ρ. The temperature dependence of the resistivity is fit in Arrhenius type equation

$$\log_e \rho = \frac{E_g}{2K_T} - \log_e K \tag{16}$$

and the measured values are plotted logarithmically as a function of reciprocal of temperature. The width of the energy gap is determined from the slope of the curve. The voltage current measurements for each sample [$poly_{10}$, $poly_{30}$, $poly_{50}$] are carried out by reversing the polarity of the contacts for several times.

AC Conduction Process in Doped Azopolyester: Charge transport mechanism in conjugated polymers and their related materials have been of considerable interest recently because they can provide information about the structure, conductivity, current density and capacitance of their polymer materials. The transport mechanisms in polymers are very much dependent on defects in polymer chains and dopant ions. A main distinguishing feature between AC and DC conduction is that in the former, it is necessary to transfer a charge between a pair of states, whereas in the later a continuous percolation path between electrodes is necessary for the current to flow. AC conductivity exhibits a common behavior in many disparate materials which can be represented as a power law dependence of the conductivity on frequency.

$$\sigma_{ac}(\omega,T) = A\omega^s \tag{17}$$

where σ_{ac} is the AC conductivity, A is a constant, ω is the angular frequency *(=2 πf)* and 's' is the exponent of the frequency component generally less than (or) equal to unity.

Correlated Barrier Hopping (CBH)

Model for AC conduction: The AC conductivity of doped Azopolyester arises because the AC conductivity is often dominated by electron states deep within the main energy gap, in the region of the Fermi level. Such deep defect states are invariably associated with the irregularities and discontinuities of the amorphous atomic network and have a strong influence on the properties of these materials[8].

The AC conductivity of the material is calculated by two distinct models, namely Quantum Mechanical Tunneling (QMT) and Correlated Barrier Hopping (CBH) model. The popular model to find the AC conductivity is CBH model. Here the term 'hopping' is used for thermal activation of charge carrier of a pair over the potential barrier between the states. If we consider a single electron hopping between size pairs over the potential defect centers then the potential barrier will be reduced by the Coulomb interaction shown in Figure 4.

The barrier height 'w' is correlated with the separation R according to the relation

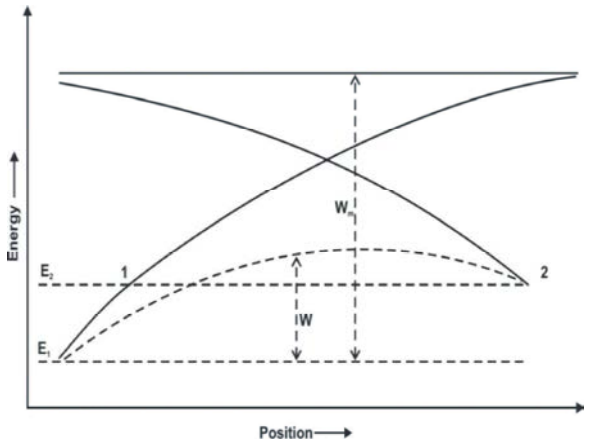

Fig. 4: Parameters for a CBH hopping between states 1 and 2

$$W = W_m - \frac{\eta_e^2}{\pi\varepsilon\varepsilon_o R_{12}} \quad (18)$$

where $\epsilon\epsilon_o$ is the background permittivity of the semiconductor, R is the separation between the neighboring sites 1, 2 and W is the hopping barrier potential after lowering of effective barrier (W_m) due to Coulomb wells overlap and 'n' is the number of charge carriers involved in hopping process. The frequency dependence of σ_{ac} in the form of equation (17) can be deduced using the relation.

$$S = \frac{d\ln\sigma_{ac}(\omega)}{\alpha\ln\omega} \quad (19)$$

For single – electron Coulomb reduced barrier (equation 18) the equation for frequency exponent's' is of the form

$$S = 1 - \frac{6k_T}{W_m + k_T ln(\omega\tau_o)} \quad (20)$$

Here's' is predicted to decrease from unity with increasing temperature and the initial decrease will be linear with temperature. The relaxation time 'τ' for the charge carrier to hop over the barrier of height 'ω' is given by

$$\tau = \tau_o \exp\left[\frac{\omega}{k_B T}\right] \quad (21)$$

where τ_o is the inverse phonon frequency (10^{-13}S) and k_B is the Boltzmann constant (1.38054x10^{-23} J/K).

Further, according to CBH model, the numerical value for the single polaron AC conductivity σ_{ac} (ω) can be calculated using the equation.

$$\sigma_{ac} = \frac{\pi^2\varepsilon\varepsilon_o NN_p w r_w^6}{6} \quad (22)$$

Similarly, the AC Conductivity due to bipolar on hopping can be calculated based on the relation.

$$\sigma_{ac} = \frac{\pi^2\varepsilon\varepsilon_o NN_p w R_w^6}{6}\exp\left[\frac{e^2}{4\varepsilon\varepsilon_o k_B T_g R_w}\right] \quad (23)$$

Where N is the total density of charged defect states, N_P is the number of pairs contributing to AC conduction, T_g is the glass transition temperature and r_W and R_w is the optimum hopping range in single and bipolar on cases are defined as follows.

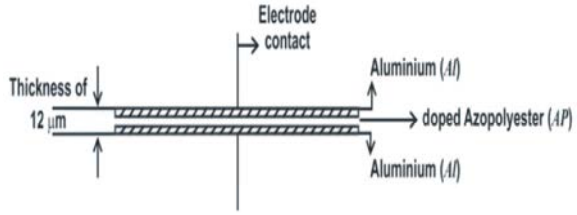

Fig. 5: Al-AP-Al sandwich system to form capacitor structure

$$r_w = \left[\frac{e^2}{\pi\varepsilon\varepsilon_o w_m}\right]\left[1 + \frac{k_B T}{w_m}\ln(w\tau_o)\right]^{-1} \quad (24)$$

$$R_w = \left[\frac{2e^2}{\pi\varepsilon\varepsilon_o w_m}\right]\left[1 + \frac{k_B T}{w_m}\ln(w\tau_o)\right]^{-1} \quad (25)$$

Here, the effective barrier height in bipolaron (w_m) case corresponds to the value of the optical gap of the material, which was determined by optical absorption measurements, whereas the effective barrier height in single polar on (w_m) case is treated as an adjustable parameter whose value can be less than (or) equal to half of the band gap value [9].

AC Measurement Techniques: For AC conduction measurements, the three different doped Azopolyester thin films of same thickness of 12μm are formed by solution casting technique, rectangular samples of polymers (2.5 cm x 3.5 cm) were used, the polymer top and bottom electrodes are deposited by Aluminum *(Al)* with the help of vacuum evaporation unit under the vacuum of 2.5x10^{-3} pa and the *(Al-AP-Al)* sandwich structure to form parallel plate capacitor which are shown in Figure 5.

Impedance, conductivity measurements are performed by using a potentionstat / Galvan stat (EG&G/PARC-Model 273A) coupled with a frequency response analyzer (Solatron Model-HF 1255) and controlled by a EG 7G/PARC software model B88 in the frequency ranging from $10H_z$-$1MH_z$. The values of resistance deduced from the data of the impedance spectrum of all the samples are observed to depend on the frequency, with the data of resistance, conductivity is found and plotted for three different doped Azopolyester. A PT 100 thermocouple connected with the temperature controller is used for maintaining the required temperature with a precision of 0.5K. The output data is transferred through GPIB interface to PC at each selected temperature and stored for further analysis.

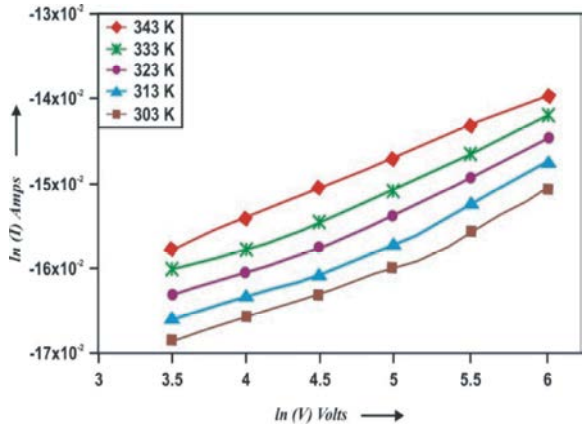

Fig. 6: Voltage current (V-I) characteristics of 10% doped Azopolyester ($poly_{10}$)

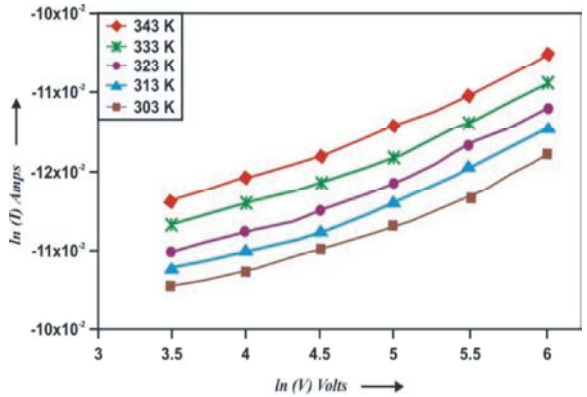

Fig. 7: Voltage current (V-I) characteristics of 30% doped Azopolyester ($poly_{30}$)

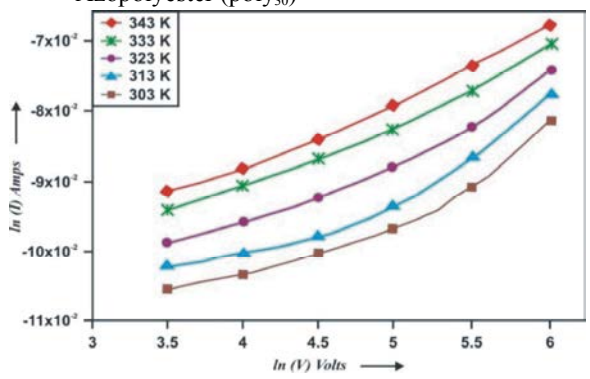

Fig. 8: Voltage current (V-I) characteristics of 50% doped Azopolyester ($poly_{50}$)

RESULTS AND DISCUSSION

The DC conduction studies of three different doped Azopolyester thin films is studied with *ln (V)* vs *ln (I)* plots of doped Azopolyester thin films at various temperature ranging from 303K - 343K which are shown in Figures 6, 7 and 8.

It is observed from figures 6, 7 and 8 that, when PANI doping percentage increases, the current increases non-linearly with applied voltage V. This is also evident from the fact that ohm's law follows from the free electron model of a metal. The free electron in a metal undergoes frequent collisions, which are not billiard – ball collisions with other electrons, but they represent the scattering of electron waves by irregularities in the crystal structure, both defects such as impurity atoms and also atoms temporarily out of place as they vibrate [10-14].

Poole–Frenkel Mechanism: The DC current-voltage relationship for Poole-Frenkel mechanism is expressed as

$$J = B\exp\left[\frac{-\phi}{kT}+\beta_{PF}E^{1/2}\right] \quad (26)$$

where

$$\beta_{PF} = \frac{e}{kT}\left[\frac{e}{\pi\varepsilon\varepsilon_0 d}\right]^{1/2} = \text{Constant} \quad (27)$$

here B is a constant. The Poole-Frenkel mechanism predicts a field dependent conductivity as

$$\sigma = \sigma_0\exp\left[\frac{\beta_{PF}E^{1/2}}{2kT}\right] \quad (28)$$

or

$$ln\sigma = ln\sigma + \left(\frac{\beta_{PF}E^{1/2}}{2kT}\right) \quad (29)$$

So that the Poole-Frenkel mechanism is characterized by the linearity of conductivity $ln\sigma$ *(mho-cm^{-1})* vs Electric field $E^{1/2}$ *(volt-cm^{-1})* plots for doped Azopolyester is shown in the Figures 9, 10 and 11.

It is observed from figures 9, 10 and 11 that the plots obey Poole-Frenkel mechanism, since there is no linearity with positive slope, it reveal that the Poole-Frenkel mechanism does not contribute significantly to the conduction as $ln\sigma$ does not show appreciable dependence on $E^{1/2}$ axis. Conductivity is increased when PANI doping percentage increases also when temperature increases, conductivity increases and it is maintained in the ranging from 70-210 Vcm^{-1}.

Fowler-Nordheim Mechanism: The Fowler-Nordheim relation (Fowler 1928) for DC current density is

$$J = AV^2\exp\left[\frac{-\varphi}{V}\right] \quad (30)$$

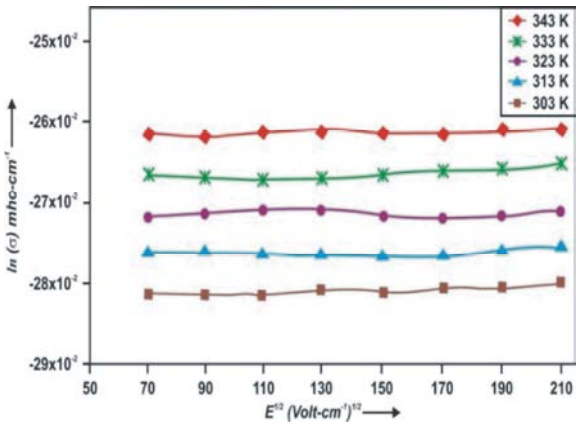

Fig. 9: Poole-Frenkel plots for 10% PANI doped Azopolyester ($poly_{10}$)

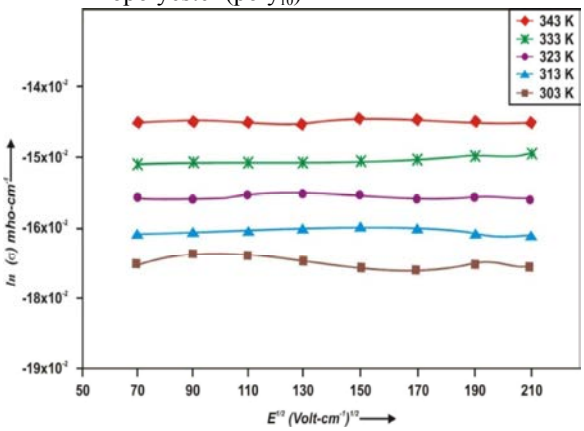

Fig. 10: Poole-Frenkel plots for 30% PANI doped Azopolyester ($poly_{30}$)

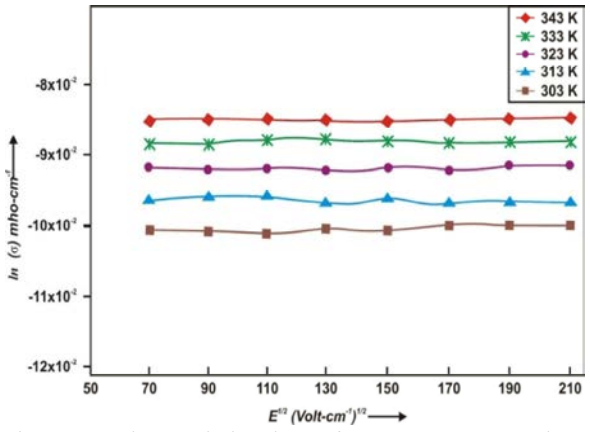

Fig. 11: Poole-Frenkel plots for 50% PANI doped Azopolyester ($poly_{50}$)

so that

$$In\left[\frac{J}{V^2}\right] = InA - \left[\frac{\varphi}{V}\right] \tag{31}$$

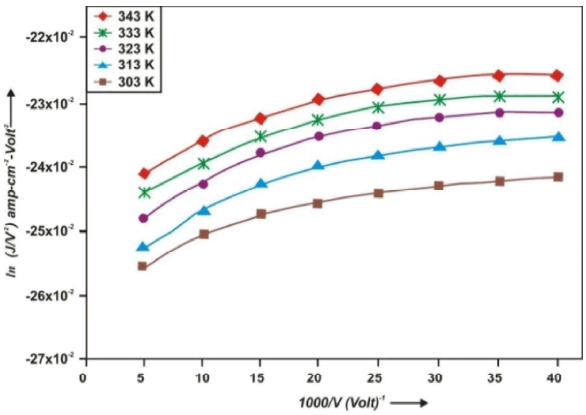

Fig. 12: Fowler Nordheim plots for 10% PANI doped Azopolyester ($poly_{10}$)

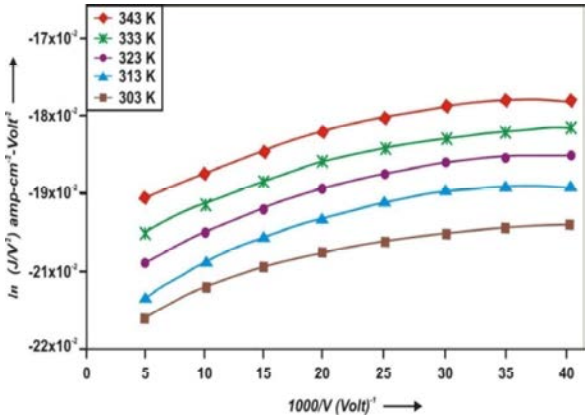

Fig. 13: Fowler Nordheim plots for 30% PANI doped Azopolyester ($poly_{30}$)

so that the $ln\ J/V^2$ vs $1000/V$ plots is expected to be a linear straight line relation with a positive slope. Figures 12, 13 and 14 shows Fowler– Nordheim plots with a range from 5 - 40 (1000/V).

In the above Figures 12, 13 and 14, the $ln(J/V^2)$ vs $1000/V$ Plots for the sample are nearly straight lines with a +ve slope for higher as well as lower values of voltage (V) indicating the absence of tunneling current as suggested by Fowler-Nordheim relation. The above figure reveals that, current density linearly increases with high PANI doping percentage in Azopolyester.

Schottky-Richardson Plots: The Schottky-Richardson current voltage relationship is expressed as

$$J = AT^2 \exp\left[\frac{-\varphi_s}{KT} + \beta_{SR}E^{1/2}\right] \tag{32}$$

$$\beta_{SR} = \frac{e}{KT}\left[\frac{e}{4\pi^2\varepsilon_o d}\right]^{1/2} \tag{33}$$

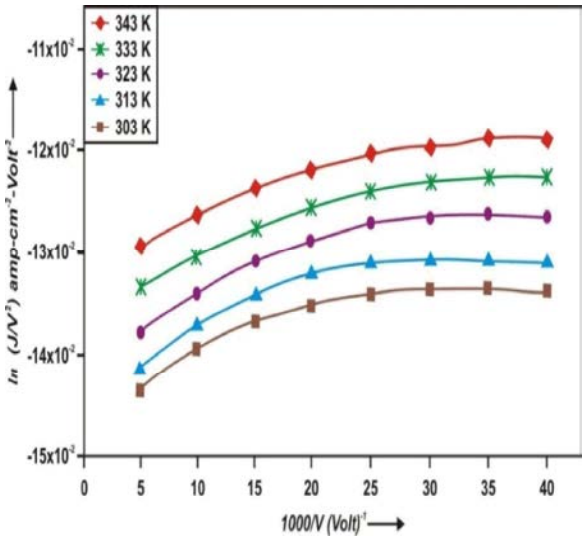

Fig. 14: Fowler Nordheim plots for 50% PANI doped Azopolyester (poly$_{50}$)

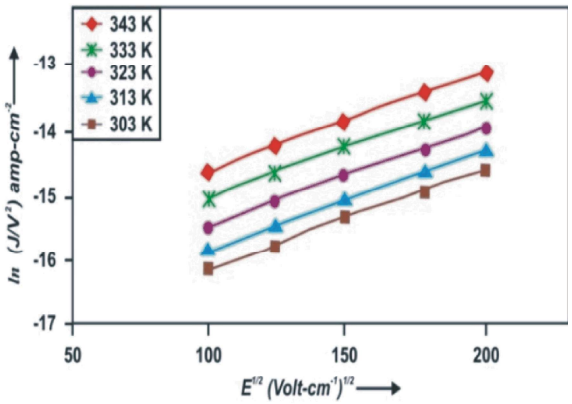

Fig. 15: Schottky plots for 10% PANI doped Azopolyester (poly$_{10}$)

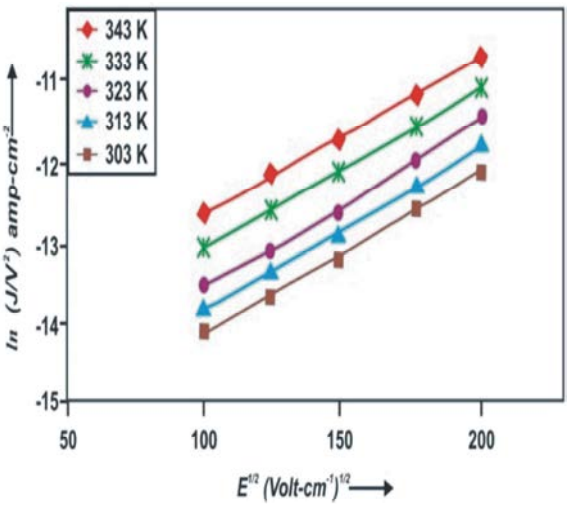

Fig. 16: Schottky plots for 30% PANI doped Azopolyester (poly$_{30}$)

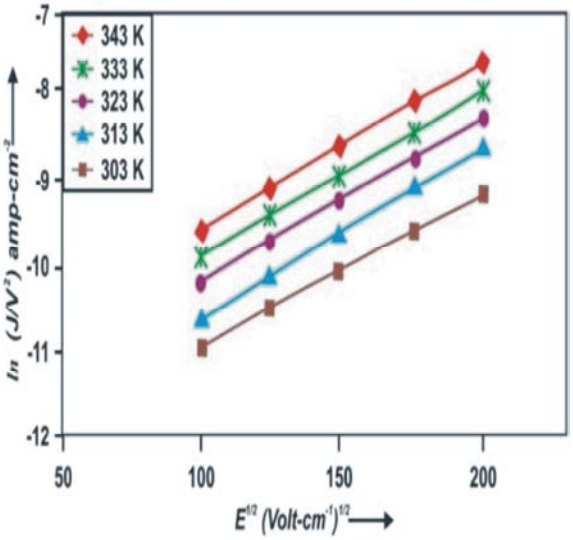

Fig. 17: Schottky plots for 50% PANI doped Azopolyester (poly$_{50}$)

and hence $ln\ J = ln\ AT^2 - \phi_s/KT + \beta_{SR}E^{1/2}$ and that $ln\ J$ vs $E^{1/2}$ plots should be a straight line with a +ve slope. The results plotted with axes marked in this way one referred to as Schottky plots and linear positive slope on Schottky plots generally characterize Schottky-Richardson mechanism. Schottky plots for the Figure 15, 16 and 17 are near straight lines with positive slope indicating that the doped Azopolyester obey the mechanism. Further, in the case of Schottky-Richardson mechanism the current shows strong temperature dependence but not in the case of the Poole-Frenkel mechanism. The study of temperature dependence of current density (J) is therefore of great importance in doped Azopolyester. The Figures 15, 16 and 17 explain Schottky Plots for three different doped Azopolyester materials with range from 100-200 $E^{1/2}$ (Volt-cm^{-1})$^{1/2}$.

The above Schottky plots reveal that current density increases when PANI doping percentage increases as well as voltage increases current linearly increases and it forms straight line nature indicating that doped Azopolyester obeys Schottky-Richardson mechanism.

Arrhenius Plots: The temperature dependence of conductivity of doped Azopolyester thin film presented in the form of Arrhenius plots is shown in Figures 18, 19 and 20 for *ln (σ)* versus *1000/T* plots at all values of applied voltage, showing a straight line with a negative slope. From the slope of the straight line, the activation energy is calculated and found to be in neighborhood of 0.71 eV.

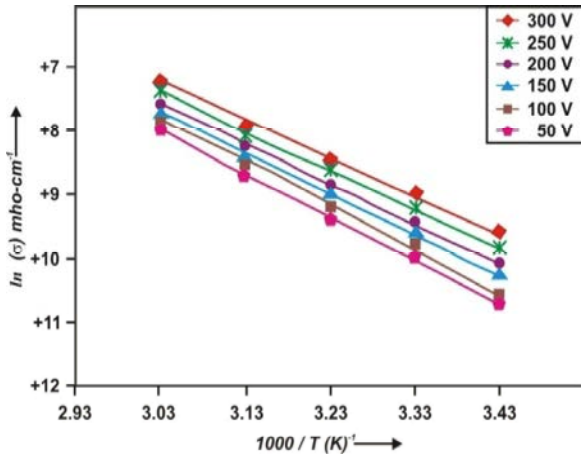

Fig. 18: Arrhenius plots for 10% PANI doped Azopolyester ($poly_{10}$)

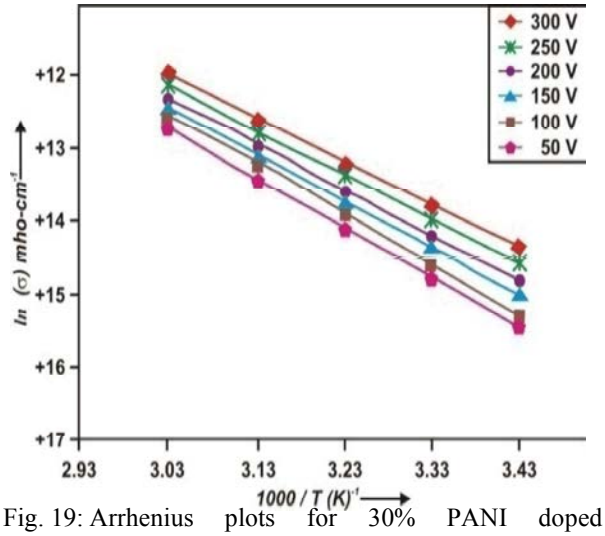

Fig. 19: Arrhenius plots for 30% PANI doped Azopolyester ($poly_{30}$)

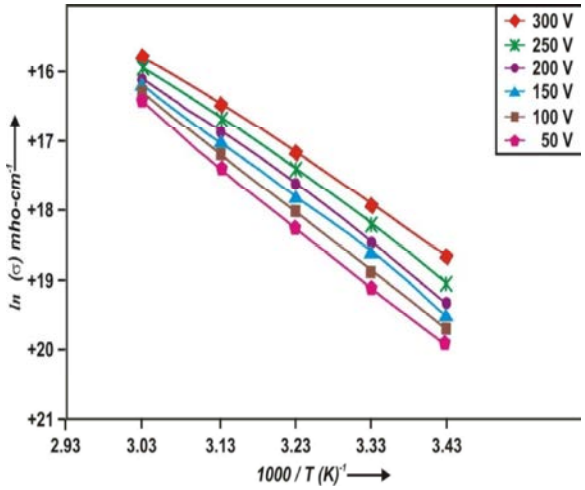

Fig. 20: Arrhenius plots for 50% PANI doped Azopolyester ($poly_{50}$)

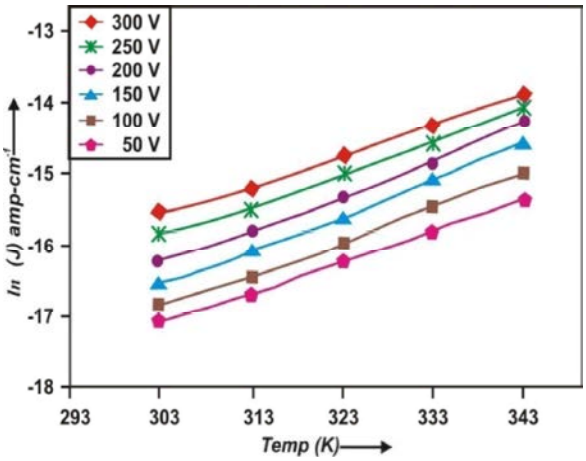

Fig. 21: Current density versus temperature plots for 10% PANI doped Azopolyester ($poly_{10}$)

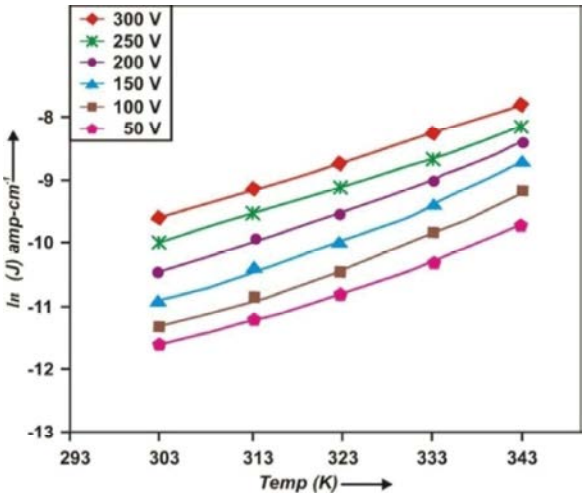

Fig. 22: Current density versus temperature plots for 30% PANI doped Azopolyester ($poly_{30}$)

Current Density Versus Temperature Plots: The temperature dependence of DC current density presented in the form of *ln (J)* vs temperature plots is shown in Figures 21, 22 and 23 and it reveal that the *ln (J)* increases linearly with temperature. The strong temperature dependence is in agreement with the Schottky-Richardson mechanism. Further, the straight line with constant slope is observed for all the fields indicating that the absence of any thermodynamic transition in the temperature range is studied.

The above three plots reveal that the PANI doping percentage and temperature increases in Azopolyester results in current density increases and it fits Schottky-Richardson mechanism.

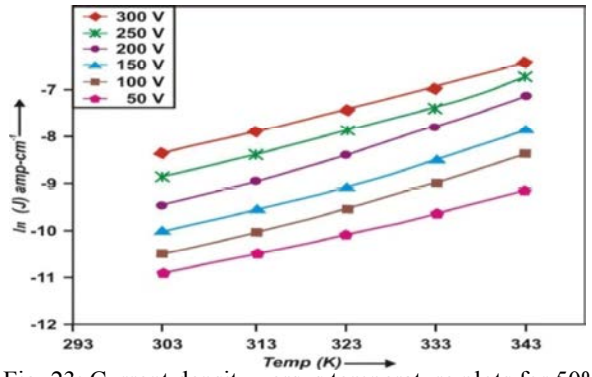

Fig. 23: Current density versus temperature plots for 50% PANI doped Azopolyester ($poly_{50}$)

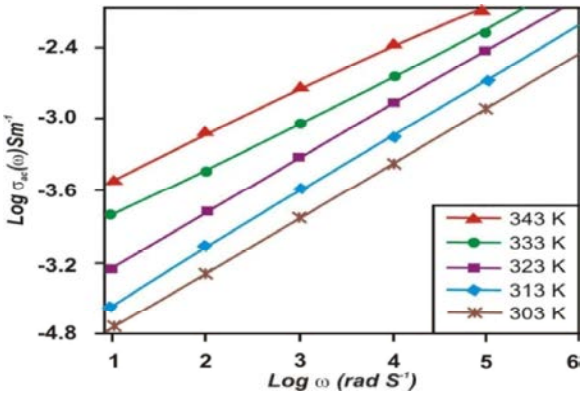

Fig. 24: Dependence of AC conductivity (σ_{ac}) as a function of frequency (w) in the temperature ranging from 303-343k for 10% PANI doped Azopolyester ($poly_{10}$)

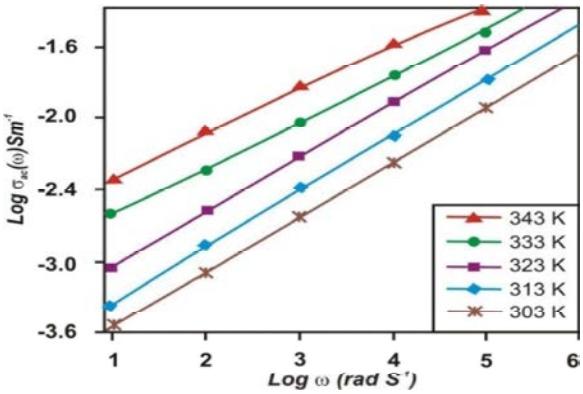

Fig. 25: Dependence of AC conductivity (σ_{ac}) as a function of frequency (w) in the temperature ranging from 303-343K for 30% PANI doped Azopolyester ($poly_{30}$)

Temperature Dependence of AC Conductivity on Frequency: The figures 24 and 25 shows the temperature dependence of AC conductivity (σ_{ac}) on frequency for three different doped Azopolyester studied in the temperature ranging from 303-343K. Within this temperature range and for a wide range of frequencies ($10H_z$- $1MH_z$) σ_{ac} takes the form of a power law equation [$\sigma_{ac}(w,T) = Aw^S$]. In the low frequency range, σ_{ac} is strongly depending on the absolute temperature while for high frequencies it becomes temperature independent.

This behavior is attributed to the time constant of the high frequency AC stimulation, which is too short for the charge carrier to relax, thus give rise to the temperature independent conductivity. In the case of CBH model, the exponent's' decreases with increasing temperature. The experimental data into the complex admittance, the following equation was used.

$$Y^* = \left(Z^*\right)^{-1} = y' + jy'' \tag{34}$$

where Y* is the complex admittance, Z* is the complex impedance, y' and y'' are respectively, the real and imaginary admittance and $j = \sqrt{-1}$.

For calculating conductivity within the range of frequency of the experiments it is found to be

$$Y^* = \left(Z^*\right)^{-1} = jwc_o\varepsilon^* \tag{35}$$

where C_o is the vacuum capacitance, w is the angular frequency and ϵ* is the complex permittivity.

CONCLUSION

It is observed from electrical studies AC conductivity of the polymeric blend films obeys the correlated barrier hopping (CBH) model and the solid lines are the straight line fits obtained by the least squares fitting procedure results. When the frequency increases conductivity also increases.

REFERENCES

1. Zuo, F., M. Angelopoulos, A.G. MacDiarmid and A.J. Epstein, 1989. Conducting polymer studies, Phys Rev B, 39(6): 3570-3577.
2. Raghunathan, A., G. Rangarajan and D.C. Trivedi, 1996. NMR, XRD, DC and AC electrical conductivity of aromatic acids doped polyaniline, Synthetic Material, 81: 39-45.
3. Kahol, P.K., 2000. Conducting polymer properties, Phys Rev. B., 62: 13803-13808.

4. Friend, R.H., 1993. Conjugated polymers and related materials, Oxford University Press, Oxford, pp: 285-296.
5. Wan, M.X., A.G. MacDiarmid and A.J. Epstein, 1987. Self assembled polyaniline nanostructures with photo isomerization function, Solid State. Science, 76: 216-222.
6. Hayashi, T., Y. Hirai, H. Tanaka and T. Nishi, 1987. Electrical investigation of polymer films, Journal of Physics, 26L: 1800-1808.
7. Kahol, P.K., R.P. Perera, K.K. Satheesh Kumar, S. Geetha and D.C. Trivedi, 2003. Electron localization length in polyaniline, Solid State Communication, 125: 369-375.
8. Reghu, M., C.O. Yoon, D. Moses, P. Smith, A.L. Heeger and Y. Cao, 1994. Transport in polyaniline networks near the percolation threshold, Phys. Rev., 50: 13931-13935.
9. Prem Nazeer, K., Sheeba Anu Jacob, M. Thamilselvan, D. Mangalaraj, K. Narayandass Sa and Y.I. Junsink, 2004. Space charge limited conduction in polyaniline films, Poly. Inter., 53: 898-905.
10. Sibghatullah Nasir, 2013. Microfinance in India Contemporary Issues and Challenges. Middle-East Journal of Scientific Research, 15(2): 191-199.
11. Mueen Uddin, Asadullah Shah, Raed Alsaqour and Jamshed Memon, 2013. Measuring Efficiency of Tier Level Data Centers to Implement Green Energy Efficient Data Centers, Middle-East Journal of Scientific Research, 15(2): 200-207.
12. Hossein Berenjeian Tabrizi, Ali Abbasi and Hajar Jahadian Sarvestani, 2013. Comparing the Static and Dynamic Balances and Their Relationship with the Anthropometrical Characteristics in the Athletes of Selected Sports, Middle-East Journal of Scientific Research, 15(2): 216-221.
13. Anatoliy Viktorovich Molodchik, 2013. Leadership Development. A Case of a Russian Business School, Middle-East Journal of Scientific Research, 15(2): 222-228.
14. Meruert Kylyshbaevna Bissenova and Ermek Talantuly Nurmaganbet. The Notion of Guilt and Problems of Legislative Regulations of its Forms. The Notion of Guilt in the Criminal Law of Kazakstan, Middle-East Journal of Scientific Research, 15(2): 229-236.